This is an original manuscript / preprint of an article published by Taylor & Francis in JOURNAL OF MICROENCAPSULATION on 27 Jun 2019, available online https://www.tandfonline.com/doi/full/10.1080/02652048.2019.1633433

Development of a continuous reactor for emulsion based microencapsulation of hexylacetate with a polyuria shell

Sven R. L. Gobert[a]*, Marleen Segers[a], Stijn Luca[b], Roberto F. A: Teixeira[c], Simon Kuhn[d], Leen Braeken[a,d], Leen C. J. Thomassen[a,d]

[a]*Faculty of Industrial Engineering, KU Leuven , Diepenbeek, Belgium*

[b]*Ghent University, Department of Data Analysis and Mathematical Modelling, Gent, Belgium*

[c]*R&D, Devan Chemicals, Ronse, Belgium*

[d]*Department of Chemical Engineering, KU Leuven, Leuven, Belgium*

*Corresponding author. Tel.: +321180336. E-mail: sven.gobert@kuleuven.be (S.R.L. Gobert).

This is an original manuscript / preprint of an article published by Taylor & Francis in JOURNAL OF MICROENCAPSULATION on 27 Jun 2019, available online https://www.tandfonline.com/doi/full/10.1080/02652048.2019.1633433

Development of a continuous reactor for emulsion based microencapsulation of hexylacetate with a polyuria shell

Microcapsules, enclosing active ingredients in a protective shell, are important high added-value products for pharmaceuticals, foods, textiles, and other applications. In this work, the encapsulation of an ester core with a polyuria (PU) shell is performed in flow. This is done in a continuous two stage process, including droplet generation followed by polymerisation to form core-shell microcapsules. An emulsion template is generated using static mixers, screen type and Kenics®, in a recirculation loop whereby the recycle pump shear forces are considered. The subsequent curing is performed in a classical coiled tube reactor with two geometric configurations. The quality of the emulsion is assessed through number-based capsule size distributions, and the core content. A continuous setup is achieved for PU microcapsules containing hexyl acetate with a production rate of 198 g dry capsules per hour, and a mean capsule diameter of 14.3 µm with a core content of 56.1 wt%.

Keywords: microencapsulation, interfacial polymerisation, flow reactor, static mixer, recirculation loop

Subject classification codes: include these here if the journal requires them

Introduction

Microcapsules consist of a core surrounded by a protective shell. The core material can be a solid mass (particle), a liquid droplet or a combination of both (Bansode et al., 2012). The diameter of these spherical capsules ranges from one micrometre up to one millimetre. A diameter lower than 1 micrometre, capsules are termed nanocapsules and above a diameter of 1 mm, macrocapsules (Jyothi *et al.*, 2010; Singh *et al.*, 2010). The shell material, which surrounds and protects the core, functions as a dispensing unit, releasing the core material when triggered by an external factor. Depending on the

application of the microcapsules, this can be to dissolve, to break under pressure, to protect or to induce slow release of the core material (Singh *et al.*, 2010; Bansode *et al.*, 2012). Microcapsules have become increasingly important for a wide variety of industrial sectors to the application. This includes textiles, for the incorporation of perfumes into fabric (average size 10µm) (Rodrigues et al., 2009), nutraceuticals, for the incorporation of vitamins (Schrooyen, van der Meer and De Kruif, 2001) and probiotics (size range 10-1000µm) (Martín et al., 2015) in food, pharmaceuticals, that use microcapsules for controlled drug release (diameter range 3-800µm) (Singh *et al.*, 2010; Gupta and Dey, 2013), thermal storage applications, which focuses on the encapsulation of phase change materials (size range 0.1-5µm) (Al Shannaq and Farid, 2015) and self-healing materials, whereby microcapsules filled with reactive polymers are incorporated into plastics and coatings (diameter range 40-500 µm) (Wu, Meure and Solomon, 2008; Then, Seng Neon and Abu Kasim, 2011; Nesterova *et al.*, 2012). The capsule range of interest in this article is 10-20 µm.

The development of microcapsules is mainly performed in lab-scale batch equipment. Scaling these batch reactors is difficult due to mass and heat transfer limitations and requires several steps between lab scale (g/h) and production scale (100 kg/h) (Wiles and Watts, 2008). On the contrary, flow reactors show improved mass and heat transfer properties compared to batch reactors and are therefore more scalable, keeping heat and mass transfer properties constant without the need for re-optimization on a larger scale (Jensen, 2001), (Hessel, 2009). Furthermore, by applying stationary continuous processing, the variation of the end product will be reduced compared to batch processes (Wiles and Watts, 2008).

To obtain microcapsules with a liquid core, several chemical techniques for microencapsulation have been developed based on emulsions as capsule template. The three main chemical methods are coacervation, in-situ polymerization and interfacial polycondensation (Jyothi et al., 2010). Coacervation is based on the separation of a colloidal phase from a polymeric solution, through a change in pH, ionic strength, temperature or the addition of an anti-solvent. A three phase system is formed in which the colloidal liquid in the continuous phase settles on the droplet surface (dispersed phase) followed by polymerization to form a shell around the core droplet (Jyothi et al., 2010), (Dobetti and Pantaleo, 2002). During in-situ polymerization the shell material is present in the continuous phase as a pre-polymer. As the polymerization continues, the molecular weight of the polymer increases and polymer material settles on the droplet surface forming a shell (Jyothi et al., 2010). An example of in situ polymerization is the formation of melamine formaldehyde microcapsules (Alič, Šebenik and Krajnc, 2012; Merline, Vukusic and Abdala, 2013). Interfacial polymerization entails that monomers forming the capsule shell are present in both phases of the emulsion. The monomers react on the droplet surface i.e. the interphase, to form the shell (Nesterova, Dam-johansen and Kiil, 2011). Examples of shell material are, polyester, polyamide, polyurethane or polyuria (Kondo and van Valkenburg, 1979). In general these chemical microencapsulation processes consist of two consecutive steps. Initially an emulsion is formed, which will determine the capsule size distribution. Next, a curing process solidifies the shell, sealing the core material into a capsule. The main challenge of this emulsion based microencapsulation is producing an emulsion template with a narrow droplet size distribution. Mono-disperse droplets are desired, as it ensures uniform product quality. A measure for the spread of the droplet size distribution is the relative

spread or covariance (CoV) which is the standard deviation divided by the mean capsule diameter of a number based distribution curve. There are several flow devices that are successful in creating quasi mono-disperse microcapsules. These are microfluidics and flow focusing (CoV < 3%), micro channel emulsification (CoV < 5%) and membrane emulsification (10% < CoV < 20%) (Vladisavljević, Kobayashi and Nakajima, 2012). In microfluidic devices, droplets are generated through a single capillary nozzle and encapsulated individually, resulting in narrow droplet size distribution. They operate in dripping mode which results in low production streams up to 104 droplets per second (Vladisavljević, Kobayashi and Nakajima, 2012). Microchannel emulsification (MCE) uses an array of micro channels with dimensions of 6 - 12 µm width, 4 – 7 µm depth and 25 - 140 µm in length (Sugiura, Nakajima and Seki, 2002; Vladisavljević, Kobayashi and Nakajima, 2012). The oil phase is pushed through the micro channels into the continuous phase. Membrane emulsification (ME) follows a similar process but makes use of membranes, like Shirasu porous glass (SPG) (Yamazaki et al., 2002). The droplet diameter is dependent on the pore size, which is often in the range of 0.05 to 30 µm. An adaptation of ME is the use of micro sieves, which have uniform pores. The droplet size distribution produced through ME is influenced by a large number of factors as there are transmembrane pressure, cross-flow velocity, dispersed phase flow rate, membrane and emulsifier properties (Leal-Calderon, Schmitt and Bibette, 2007). The main drawback of flow focusing, MCE and ME processes is that they are still limited in throughput (volume flow rate), making them commercially less viable (Abrahamse et al., 2002; Wagdare et al., 2010). The scale up strategy for these types of flow devices is often numbering up (i.e. placing several flow reactors in parallel), but

this is sensitive to maldistribution of the feed flow to the nozzles or channels (Jeong, Issadore and Lee, 2016).

Other means of creating liquid-liquid emulsions are active and passive mixers. Active mixers such as rotor stator mixers, colloidal mills and ultrasound transducers require an external energy source. These devices can mix large quantities (100 – 20,000 L/h), but have a CoV largely exceeding 30% (Jeong, Issadore and Lee, 2016). Passive mixers induce mixing through the energy supplied by the feed pumps. Static mixers consist out of a structure fixed in the flow path that creates complex mixing patterns (Theron and Sauze, 2011). The absence of moving parts leads to low energy costs and maintenance requirements (Theron, Le Sauze and Ricard, 2010). A large variety of static mixers have been engineered and used in emulsification processes. They are discussed in detail elsewhere (Thakur, Vial and Nigam, 2003). A few extensively studied mixers in literature are the Shulzer SMX and SMV ((Legrand and Moranc, 2001; Meijer, Singh and Anderson, 2012; Das, Hrymak and Baird, 2013)), the Kenics® static mixer ((Hobbs and Muzzio, 1997, 1998)) and the screen type mixer ((Azizi and Al Taweel, 2011; Hweij and Azizi, 2015)). These studies focus on the generation of oil in water emulsions, whereby parameters such as hold-up (ratio of dispersed phase to total volume of emulsion), dispersed phase concentration $\phi_{emulsion}$, viscosity of continuous and dispersed phase, and the number of static mixers are investigated (Fradette et al., 1996; Das et al., 2005; Theron, Le Sauze and Ricard, 2010; Kiss et al., 2011). In most studies of emulsification behaviour, the main focus is on modelling predictive formulas for droplet size. Often a model system, oil and water phase, without encapsulation application is used at low to intermediate dispersed phase concentrations (1-20 vol%) in order to avoid droplet coalescence (Paul, Atiemo-obeng and Kresta,

2004). In cases of microencapsulation, the curing is done in batch after the emulsion is collected. For industrial relevant applications, the dispersed phase concentration ratios are preferably above 20 vol% (Paul, Atiemo-obeng and Kresta, 2004) and would benefit from a continuous curing process. Theron (2012) addressed both issues in a study of the encapsulation of cyclohexane in a polyuria (PU) shell in a continuous reactor (Theron et al., 2012). In the setup, gear pumps are used to recirculate the oil and water phases from a single holding tank. This means the two phases are in contact before they pass through a SMX static mixer in the recycle loop. In the presented reactor setup of this paper, two separate feed streams of continuous and dispersed phase are implemented. First contact between the two phases occurs in the mixing zone. This avoids reagents like isocyanides (monomer for polyuria shell synthesis) to react too early with water from the continuous phase. After the emulsion is generated it is diverted into a residence time reactor where the polymerization initiator is added and curing takes place at elevated temperatures. The process was able to run with high dispersed phase concentrations of 25 vol% at a total flow rate of 163 ml/min. Other static mixers have yet to be tested in this type of reactor setup.

In the current study the emulsion template for a microencapsulation process, polyuria shell and ethyl acetate core, based on interfacial polycondensation is generated in a recirculation loop. The curing step is performed in a coiled tubular reactor. The static mixers investigated are a Kenics® static mixer and a screen type mixer. These mixers have very different geometries resulting in distinctive flow behaviour. The Kenics® static mixer shows droplet breakup due to shear forces, induced by the fluid streams, exceeding the interfacial tension force (Farzi, Mortezaei and Badiei, 2010). As the flow rate increases, the shear forces are enhanced, resulting in smaller droplet

diameters (Farzi, Rezazadeh and Nejad, 2016). The screen type mixer consists out of woven screens placed perpendicular to the flow direction. Although droplets can break-up into smaller ones on impact with the screen structure, the main droplet breakup occurs through turbulent mixing directly after the screen (Azizi and Al Taweel, 2011). The fluid passing the cylindrical wires of the screens forms jet streams that converge into a uniform flow (Azizi and Al Taweel, 2011). These uniform hydrodynamic flow conditions generated by the screen type mixer make it an interesting static mixer for emulsion based microencapsulation studies, which, to the authors knowledge, has not been investigated so far.

The novel aspect of the current setup is the fact that the emulsion is not created semi-batch wise. Instead both phases of the emulsion are pumped continuously into the recirculation loop where first contact of the phases occurs. The input and exit flow rates are identical. A study is performed on the mixer geometry for identical diameters, static mixer volume and the superficial velocity inside the loop. Results are discussed in terms of the mean capsules diameter and spread of the capsule size distribution.

Materials and Methods

Microencapsulation

The microencapsulation method used is based on an oil-in-water interfacial polycondensation, whereby a diphenyl methane diisocyanate (MDI) trimer reacts with triaminopyrimidine, forming a polyuria shell (Nguyen et al., 2015). The continuous phase of the emulsion is a 13 wt.% arabic gum solution (AG) (Sigma-Aldrich, Saint Louis, Missouri, US) prepared in ultrapure water. The dispersed phase contains

hexylacetate (HA) (99% purity, Sigma-Aldrich, Saint Louis, Missouri, US) combined with a MDI based prepolymer, Suprasec® 2030 (Devan Chemicals, Ronse, Belgium), as the first monomer. The shell of the droplets is formed by adding the second monomer, 2,4,6-triaminopyrimidine (TAP) (Sigma-Aldrich, Saint Louis, Missouri, US). The TAP solution is added to the emulsion in a volume ratio of 4.8:10.

Two important process parameters are defined, the dispersed phase concentration of the emulsion, $\phi_{emulsion}$, and the microcapsule concentration of the exit stream, $\phi_{microcapsules}$:

$$\phi_{emulsion} = \frac{Q_{oil\ phase}}{Q_{emulsion}} \quad (1)$$

$$\phi_{microcapsules} = \frac{\phi_{emulsion} Q_{emulsion}}{Q_{total\ outlet}} \quad (2)$$

The emulsion concentration is the ratio of oil phase to the total amount of emulsion, in a batch experiment this is a volume ratio, and in flow this ratio is determined through the ratio of feed flow rate, Qoil phase, to the total feed flow rate, Qemulsion. For all experiments this ratio is kept constant at 28.8 vol%. The microcapsule concentration is the ratio of the feed flow rate of oil phase (determined by the dispersed phase concentration multiplied with the feed flow rate) to the total flow rate at the reactor outlet. It also determines the amount of end product generated, a higher microcapsule concentration means more capsules per millilitre at the reactor exit. During the flow experiments the addition of the polymerisation initiator is done in two different ways in order to change the microcapsule concentration. As shown in **Fout! Verwijzingsbron niet gevonden.**, the total exit stream consists of the flow of emulsion coming from the recirculation loop (sum of oil and water phase feed flows) and the flow of TAP solution

added after the emulsification in the recirculation loop. The microcapsule concentration in this setup with post-emulsification addition of TAP is 19.5 vol%. The TAP can also be directly dissolved in the arabic gum phase (water phase of emulsion) at the beginning, before the emulsion is formed in the recirculation loop, i.e. pre-emulsification addition of TAP. The shell formation reaction is slow at room temperature and will not hinder the emulsification in the recirculation loop. In doing so the TAP feed after the recycle loop is no longer needed and the reactor outlet flow rate is the same as the feed flow rate of emulsion, leading to a capsule concentration of 28.8 vol%.

Emulsification

The emulsification in batch protocol uses an Ultra Turrax T 18 (IKA) high shear mixer at 7600 rpm. In flow the emulsification is performed in a recirculation loop as shown in **Fout! Verwijzingsbron niet gevonden.**, under different superficial flow rates. In these experiments curing is performed in batch. All feed streams of reagents are supplied by peristaltic pumps (Watson & Marlow, Fluid Technology Group, Falmouth, UK, model 120 U/DV), indicated by (1a,b,c) in **Fout! Verwijzingsbron niet gevonden.**. The continuous feed flow rate of emulsion is fixed at 15 ml/min. The feeds (1a and 1b) are pre mixed in a Y-mixer leading to a coarse emulsion (droplets of 2 – 5 mm in diameter) which enters the loop via a T-mixer located directly upstream of the static mixer ((2) in **Fout! Verwijzingsbron niet gevonden.**). To avoid air bubbles, the loop is filled with the coarse emulsion before each experiment. The tubing of the recirculation loop has an internal diameter of 4.8 mm. The flow within the loop is ensured by either a peristaltic pump (Verderflex vantage 3000 C EZ, Verder Ltd, Castleford, UK), a gear pump

(Ismatec Reglo-z, M0013, Cole-Parmer GmbH, Wertheim, Germany) or a centrifugal pump (Model M510S, TCS micropumps, Kent , UK) (3). Two types of static mixers: screen and Kenics® static mixer from Cole-Parmer (Metrohm Belgium n.v., Antwerp, Belgium) are used, both having an internal diameter of 6.8 mm and placed directly after the feed entrance point (T-mixer) of the emulsion. This ensures the entering fluid passes the static mixers at least once. The Kenics® static mixer is used with 13 mixing elements. The screen type mixer is custom made with 9 screens from stainless steel mesh (Omnimesh, Lokeren, Belgium), placed perpendicular to the flow direction. The mesh size (length of open square) is 265 µm and a wire diameter of 155 µm. Screens are spaced 5 mm from each other. This is close to the wire screen used by Azizi (2011) whose wire screens have a mesh size of 210 µm and 152 µm wire diameter (Azizi and Al Taweel, 2011).

The fluid entering the loop displaces the same amount of fluid toward the loop exit, **Fout! Verwijzingsbron niet gevonden.**. At the exit (Y-mixer connection) the generated emulsion is combined with the TAP solution in a Y-mixer, resulting in a total flow rate of 22.2 ml/min. Recirculation rates were varied between, 110 and 579 ml/min. The exit stream is collected for curing after 9 minutes. All Y- and T-mixers are supplied by Reichelt Chemietechnik GmbH + Co., Heidelberg, Germany.

Curing

During the emulsification experiments, to investigate the influence of superficial flow rate and shear force of the pump on the capsule size distribution (CSD), curing is done in batch. A small amount (10 ml) of the emulsion is collected in a vail and placed in a water bath at 65°C for 5 minutes. In the batch experiment 80 ml of the emulsion is

cured in an EasyMax 102 Basic synthesis reactor system (Mettler-Toledo, LLC, Columbus, US). A temperature program heats the reaction mixture from 22 to 65 °C at 3.4°C/min. The mixture is cooled in an ice bath upon reaction completion.

Figure 1 near here

Characterisation of Microcapsules

The capsule size distribution is determined with optical imaging. One droplet of sample is placed on a glass slide and diluted in one droplet of ultrapure water and stirred gently until a homogeneous mixture is obtained. A cover slip is placed on top of the sample. This direct dilution reduces capsules overlapping and aggregating, resulting in clear micrographs, Figure 2.

Figure 2 here

Microscopic images are made with an Axiocam 105 color (Carl Zeiss, Oberkochen, Germany) and with a 100x magnification (10x objective lens and 10x ocular lens). They are analysed using ImageJ (Abràmoff, Magalhães and Ram, 2004). To avoid false detection of noise (pixels or groups of pixels turned black after thresholding, due to variations in brightness of the background, caused by the liquid surrounding the capsules) capsule measurements require a minimal area consisting out of at least 10 pixels to be considered a microcapsule. This corresponds to a detection limit of particles with a diameter of 1.57 µm. A further selection of particle area is based on circularity and roundness to avoid measurements of aggregates. The resulting number based capsule size distributions are based on at least 2000 measurements of capsule diameters. The mean capsule diameter and the covariance (CoV) are quantified for each capsule size distribution.

$$CoV = \frac{\sigma}{d_{mean}} \quad (3)$$

Whereby d_{mean} is the mean capsule diameter and σ is the spread of the capsule size distribution. In the case of bimodal curves, the two modes are separated with the antimode as intersecting point. The modes and antimode are determined with the locmode function of Rstudio, which uses kernel density estimations to model the data.

For the determination of the core content microcapsule samples are filtered on a Whatman 40 filter under vacuum, and washed with a 30% ethanol solution (VWR, Radnor, Pennsylvania, US). The capsules are left to dry for 60 min at ambient temperature. Extraction of the core is done by placing 2g of the filtered capsules in an air tight vial to which 15 ml of dimethylformamide (DMF) (ucb, Leuven, Belgium) is added. The content is stirred for 48 hours. GC-FID analysis (Hewlett Packard, Palo Alto, California, US) is performed with a ZB5 column and 2-(-1-methoxy)propyl acetate is used as the internal standard (Thermo fisher scientific, New Jersey, US). The mass fraction of shell material is determined by drying a sample of 2 g of filtered capsules to constant weight in a crucible at 100 °C. During this period, complete evaporation of the core is obtained (no traces of hexyl acetate detected with GC-FID analysis of extracted dry capsules), enabling the determination of the dry shell mass of the filtered capsules. The core and the dry shell weight determination are done twofold. The percentage of the core content is determined as follows:

$$Core\ content\ (wt\%) = \frac{m_{core}}{m_{core}+m_{shell}} \quad (4)$$

Whereby m_{core} is the mass of core and m_{shell} is the mass of dried shell of empty capsules.

Flow Reactor operation

The tubular residence time reactor is made out of PTFE with an internal diameter of 4 mm (Polyfluor Plastics bv, Breda, Netherlands) and is used in two configurations. The tube is coiled with a coil diameter of 14 cm, or the tube is coiled alternatingly between two coils of 5 cm, resulting in an 8-shape. The tubular reactor is dimensioned to obtain a residence time of 6 minutes and is placed in a water bath at 65°C. The feed flow rate is fixed at 15 ml/min. The continuous exit stream is quenched directly in ice cold water.

Characterisation of the flow reactor

The flow behaviour inside the residence time reactor is characterised through the residence time distribution (RTD). When fluid elements enter a reactor, their time spent inside the reactor will depend on the path they follow. Because different elements follow different paths, there will be a spread on the residence time. This distribution of residence time is a measure of macromixing and is determined through an input-response experiment. The step-input of the reactor is a feed change from a 0.01 M KCl solution (Merk, Darmstadt, Germany), to ultrapure water at 22.2 ml/min. The conductivity of the exit stream is monitored at 1 s intervals with a micro flow cell 829-CE, Model 3082-S-CE digital conductivity meter (Amber Science Inc., Oregon, US). The resulting conductivity signal in function of time is converted to the F(t) curve, from which the mean residence time, tm, and variance, σ^2, are calculated. The RTD is also measured with the emulsion matrix. For this experiment the step input is a switch between a premade emulsion with arabic gum containing 0.1 M KCl, and in situ generated emulsion with standard Arabic gum solution. The TAP is omitted in these formulations to avoid the polymerization reaction. De experimental distributions will be

compared to the normalised dispersion model (equation 5). Ideal plug flow shows a distribution with zero spread. Flow behaviour that shows minor deviations from ideal plug flow is characterised by a symmetric bell shaped curve which can be fitted by the dispersion model, whereby Dax/uL, the dispersion number, is smaller than 0.01 (Levenspiel, 1999).

$$E_\theta = E(t).t_{res} = \frac{1}{\sqrt{4\pi\left({}^{Dax}/_{uL}\right)}} \exp\left(-\frac{(1-\theta)^2}{4\left({}^{Dax}/_{uL}\right)}\right) \quad (5)$$

The dispersion number consists out of the axial dispersion coefficient, u is the linear velocity and L is the reactor channel length. The normalised time is expressed as ɵ = t/t_{res}, with t_{res} the mean residence time.

Results and discussion

Batch

The batch process uses a rotor stator mixer, generating high shear forces to break-up droplets. Figure 3 shows a capsule size distribution curve obtained with the rotor-stator mixer for the encapsulation of hexylacetate with polyuria. Under the current conditions of 7600 rpm, the shear rate is 1.06 104 /s. The obtained capsule size distribution curve shows clearly a bimodal distribution. The first mode shows a mean diameter of 3.5 µm and a covariance of 33.1%, this peak represents 16% of the total number of capsules measured. These capsules are very small and are considered as product losses, because they are too small to have a useful amount of core material. In terms of volume fraction of material, only 0.61 % of the core material is contained in these small microcapsules. The desired microcapsules represented by the dominant second mode are 11.5 µm and

show a covariance of 25.7%. The first mode at low capsule sizes could be a result of a break-up mechanism leading to satellite droplets whereas the second mode of the distribution curve represent the larger daughter droplets. Satellite droplets can be formed by different mechanisms. The first one occurs when a mother droplet is elongated into a dumbbell shape. As the elongation reaches a limit, the mother drop breaks up into two daughter droplets at the dumbbell ends, while satellite droplets are formed in between. A second possible mechanism is tip streaming, whereby small droplets are pitched of the ends of an elongated droplet. This latter mechanism is more likely to take place at viscosity ratios $p= \mu_d/\mu_c$ much smaller than 1 (10-3- 10-2) (Tucker III and Moldenaers, 2002). As the current emulsion has a viscosity ratio of 0.6, the first mechanism seems more likely.

Figure 3 near here

Flow

Recirculation pump as an active mixer

Most pumps present a degree of mixing giving them emulsifying properties when pumping immiscible fluids. This contribution to the generation of an emulsion is investigated in three different pump types, a peristaltic, a centrifugal and a gear pump. The pump is placed in the recycle loop without static mixers. The TAP addition is done pre-emulsification. Results are expressed as mean diameter derived from number based distributions in function of the superficial flow rate inside the empty recirculation loop. All three pumps show strong emulsifying properties, but differ in type of distribution (mono- and bimodal) and in achievable range of the capsule size with superficial

velocity, Figure 4. These differences are due to the difference in pumping mechanism resulting in droplet break-up.

Within a peristaltic pump the highest shear rate, which determines droplet break-up, is induced in the smallest cross-section of the tube, i.e. the exit point where the tube is clamped in the pump head, possibly acting as a narrow gap emulsifier. Droplets could also be generated through the pulsation caused by the compression and expansion of the fluid within the pump. The distributions obtained in this pump show a bimodal character for all flow conditions. These curves are treated in the same manner as mentioned for the batch results. The contribution of the first mode (representing small capsules) increases as the flow rate increases. At the highest flow rate this is 3% of the total volume of capsules. The effects of superficial flow rate on the capsule size distribution is shown in Figure 4, where solely the second mode is considered. The peristaltic pump shows a slight (17 to 12 μm) decrease in mean capsule diameter from when the flow rate is increased while the spread of the capsule size distribution stays roughly the same. The centrifugal pump can be seen as an inline impellor, with 5 vertical blades. At the lowest flow rate a bimodal distribution is observed, whereby the first mode represents a volumetric fraction of 0.6%. As the flow rate increases, droplets of the second mode are broken up further resulting in monomodal curves. This pump shows a larger range of capsules mean diameters, varying between 20 to 6 μm over the total range of flow rates. However the spread of the capsule size distribution is large.

The gear pump uses two interlocking gears as a pumping mechanism, fluid is trapped between two teeth of one gear and the pump chamber wall and is carried from the suction side to the outlet, during which it is mixed. Fluid might be passing between the gap of the gear tooth end and the pump chamber wall, giving it a rotor-stator like

operation. At low flow rates the particle size distribution shows a peak at 16 µm and very long tailing toward large microcapsules of which 10% are above 203 µm. The resulting mean diameter is large (55.5 µm) and the capsule size distribution has a very large spread. As the flow rate increases to 0.31 m/s droplets are further broken up to very small capsules leading to a first mode at 2 µm and a second mode at 15.6 µm. A further increase in the superficial flow rate results in a further droplet break-up of the capsules of the second mode, which strongly decreases the mean diameter of the distribution and a plateau of 3 µm at superficial flow rates > 0.5 m/s is reached. At low flow rates the fluid trapped between the gears undergoes less break up leading to larger capsules. When the flowrate increases, turbulence in this fluid section also increases leading to more breakup.

The most constant performing pump is the peristaltic pump, which also shows the lowest covariance of all pumps (<40%). Even at low flow rates the mean droplet size is within the desired range. This pump is used in further investigation of the microcapsule concentrations and static mixers.

Figure 4 near here

Microcapsule concentration

The two different methods of introducing TAP to the emulsion, post- and pre-emulsion addition, which leads to different microcapsule concentrations of 19.5 vol% and 28.8 vol% respectively, are tested by generating an emulsion in a recirculation loop without static mixers operated with a peristaltic pump. Operated at the same feed flow rates the more concentrated system (28.8 vol%), delivers a higher yield of microcapsules when using pre-emulsification addition of TAP. The pre-emulsification addition leads to a

higher concentration of 0.22 g dry capsules per processed ml of emulsion, compared to 0.15 g/ml for the post-emulsification addition. The total yield of microcapsules is 3.3 g (dry weight capsules)/min, or 198 g/h, for both pre-emulsion and post emulsion addition. They are equal because of equal feed flow rates in the experiments. Figure 5 shows the mean diameter and the spread of capsule size distributions obtained after pre and post emulsification addition of TAP, Figure 5 a,b. There is little difference in the capsule size distributions. This suggest that the break-up remains the same in the recirculation loop when TAP is added to the arabic gum. At higher microcapsule concentration the coalescence of droplets is promoted, however no major increase in coalescence (increase in mean diameter) is seen after the emulsion exits the loop. This could be because a preliminary membrane is formed around the droplets upon exiting the recycle loop. This membrane formation is supported by the measurement of the interfacial tension, which strongly decreases during the first 6 minutes and reaches a constant value due to the shell formation reaction taking place. Taking into account a mean residence time of 3 min inside the recirculation loop, this gives the reaction ample time to form a thin membrane around the droplets, which aids stabilisation and hinders coalescence.

Figure 5 near here

Static mixers

To investigate whether static mixers can further increase control over microcapsule size and reduce the covariance, two types of static mixers are tested in the recirculation loop operated with a peristaltic pump. Figure 6 shows the results obtained with 13 Kenics® static mixer and 9 screen type mixers. The active mixing volume are the same for both

static mixers. Overall there is little to no difference between the capsules size distributions, i.e. mean diameter and spread stay almost the same. Only the screen type mixer is able to induce a further reduction of the spread at a high superficial flow rate. The emulsion droplet diameters are reduced in the pump to a size where they pass through the gaps of the static mixers and remain unchanged by the flow conditions within the static mixer. The peristaltic pump is the controlling mechanism for droplet breakup.

Figure 6 near here

Curing in flow

Theron (2012) highlights the need for axial mixing and a minimium of backmixing, i.e. ideal plug flow behaviour, during the curing proces of the microcapsules (Theron et al., 2012). The tubular reactors are therefore characterised through determination of the residence time distribution, with water and emulsion. The normalized residence time distribution curves are shown in Figure 7.

The flow in the single coiled tube reactor is skewed to the right, compared to the dispersion model with a D/uL of 0.01, indicating deviation from ideal plug flow due to laminar flow behaviour inside the coiled tube. The 8-shaped coil shows a very good fit with the dispersion number for a D/uL of 0.002, indicating close to ideal plug flow. The covariance of 14% in the circular coil shape is reduced to 6% in the 8-shaped tube. The alternating coil direction induces axial mixing through dean vortices, reducing the spread on the residence time, comparable to the effects in a continuous flow inverter (Klutz et al., 2015). This reactor would indicate the ideal flow conditions for a residence

time reactor in a microencapsulation process. However, water is not a good representation of the emulsion passing through the tubular reactor. When performed with emulsion, which is the actual matrix, the residence time distribution shows strong deformations in shape from the ideal dispersion model (symmetric bell-shaped curve). The coiled tube RTD shows a covariance of 22%, while the 8-shaped coil RTD shows a covariance of 17%. This indicates some reduction of spread of the RTD, but not enough to obtain ideal plug flow. Both residence time distribution measurements made with emulsion could not be modelled with the dispersion model. The differences in RTD-measurements are dependent on the fluid properties and highlight the need to incorporate the fluid matrix effects of a system into the measurement of the RTD.

Figure 7 near here

For the continuous curing experiments, the emulsion is generated in a recirculation loop operated by the peristaltic pump at 0.31 m/s with 13 Kenics® static mixer placed in the loop. The encapsulation process is tested in the single and 8-shaped coiled tubular reactor. The addition of TAP is done post-emulsification. Results of the distribution curves are seen in Figure 8. Two phenomena can be seen from the capsule size distributions. When comparing the batch cured emulsion to the emulsion cured in the coil, there is an increase in the spread of the capsule size distribution. This is due to both droplet coalescence, causing the shift of the second mode toward the right, as well as further droplet break-up, which increases the capsule count of the first mode. The second mode is shifted toward larger capsules, leading to an increase in mean capsule diameter. Laminar flow promotes droplet coalescence as it increases contact time of droplets, increasing the possibility of reaching a critical film thickness (Paul, Atiemo-obeng and Kresta, 2004). The increased droplet break-up during curing in flow could be

due to droplet-wall interaction. During the flow experiment some fouling of the tube wall is observed, indicating that polymer material from a droplet is sticking to the wall upon droplet collision. Colliding droplets could temporarily stick to the tube wall, elongate and separate to form small droplets, that in turn become microcapsules. The capsule size distribution of the 8-shaped reactor shows less coalescence than the single coiled reactor, however there seems to be more droplet break-up. The increased axial mixing ensures that droplets are surrounded by shell material and aids uniform shell formation, however it increases droplet-wall interaction, which leads to an increase in droplet break-up. Overall the volume of the first mode of the CSD is still only 1.4% of the total volume of obtained capsules.

Figure 8 near here

Core content

Batch produced capsules show a core content of 62 wt%, for capsules with a mean diameter of 11.5µm and covariance of 25.7%. Capsules produced in the recirculation loop with 13 Kenics® static mixers at 0.31m/s, show a mean capsule size of 14.3 µm and a covariance of 37.8%. The core content is 56 wt% when cured in batch and 54 wt% when cured in flow.

System performance and application ranges

An overview of emulsification devices reported in literature is presented in Table 1, which includes the process parameters, emulsion concentration and dispersed phase flow rate, and the obtained results of mean diameter and covariance. All the presented results in Table 1 are derived from number based droplet size measurements ensuring a

fair comparison of data, and only oil-in–water-type emulsification are considered. The devices in Table 1, other than the reactor currently presented, make no use of continuous curing. Theron 2012 is, to the authors knowledge, the only publication that presented continuous encapsulation in a single setup, but used volume based distributions and Sauter mean diameter to present their findings, and is therefore not comparable with the current results (Theron et al., 2012).

Devices that are able to generate almost monodisperse particles (<5%) are the microfluidic and microchannel reactors examples presented are from Nisisako (2008) and Neves (2008) respectively ((Neves et al., 2008; Nisisako and Torii, 2008). Their dispersed phase flow is low (order 10-3 L/h), and it requires large pressures to push this phase through the individual micro-sized orifices for droplet generation (Martin-Banderas, Ganan-Calvo and Fernandez-Arevalo, 2010). Membrane emulsification reactors, have more random pore structures and allow higher flow rates, but yield more polydisperse particles (11-20%) (Yamazaki et al., 2002). Larger devices like the SMX mixer tested by Fradette (1996) are operable with high flow rates (10 L/h) and achieve covariances of 20% (Fradette et al., 1996). The tested dispersed phase flow rate in this work performs similar to the static micro mixer of Whiske (2006), and is situated in the range between membrane emulsification and microfluidics. However the current setup yields a larger covariance (>30%) compared to the other emulsification devices. This has been proven to be the result of the pump in the recirculation loop, as it dominates the emulsification and is not designed to deliver homogenous shear forces to generate droplets. Furthermore a high emulsion concentrations as used in the present system (>20%) increases collisions between droplets (Paul, Atiemo-obeng and Kresta, 2004) and droplet-wall interaction, which can lead to more polydisperse emulsions.

The advantage of the current setup offers the possibility to generate emulsions where feed flow rates of disperse or continuous phase have no direct influence. This is in contrast to the other listed devices where an increased production rate will affect obtainable droplet size and increase covariance. The presented device realizes this through a fast recirculation part with high flow rates, followed by a reduced flowrate for the curing stage reaction step. Future work will focus on finding the maximum feed flow rate, whereby the recirculation loop is flushed out, and droplet breakup is limited due to the reduced residence time in the loop. Further improvements are to be made to the recirculation loop, whereby an inline rotor stator mixer could offer both emulsification and fluid circulation.

Table 1 near here

Conclusions

A continuous setup for the microencapsulation of ethyl acetate with a polyuria shell is developed. The production rate of capsules, with a mean diameter of 14.3 µm, is 198 g (capsules)/h with an average ethyl acetate core content of 54 wt.%. The emulsification is performed in a recirculation loop reactor and a high microcapsule concentration was implemented by adding the polymerisation initiator for the interfacial polymerisation directly in to the water phase of the emulsion prior to the emulsification. The driving pump of the recirculation loop determines the range of capsule size and its distribution. With a peristaltic pump, the addition of the Kenics® or screen type static mixers shows no influence on the mean capsule diameter nor the spread of the capsule size distribution. The covariance of the system can still be improved, by implementation of a rotor stator mixers instead of a pump. This will be considered in future work to produce

large amounts of emulsion and achieve a relevant low covariance.

Acknowledgment

The author would like to thank Devan Chemicals for their support. This work was performed with internal KU Leuven funding StG/15/029.

References

Abrahamse, A. J., Van Lierop, R., Van der Sman, R. G. M., Van der Padt, A. and Boom, R. M. (2002) 'Analysis of droplet formation and interactions during cross-flow membrane emulsification', *Journal of Membrane Science*, 204(1–2), pp. 125–137. doi: 10.1016/S0376-7388(02)00028-5.

Abràmoff, M. D., Magalhães, P. J. and Ram, S. J. (2004) 'Image processing with imageJ', *Biophotonics International*, 11(7), pp. 36–41. doi: 10.1117/1.3589100.

Ališ, B., Šebenik, U. and Krajnc, M. (2012) 'Microencapsulation of butyl stearate with melamineformaldehyde resin: Effect of decreasing the pH value on the composition and thermal stability of microcapsules', *Express Polymer Letters*, 6(10), pp. 826–836. doi: 10.3144/expresspolymlett.2012.88.

Azizi, F. and Taweel, A. M. Al (2011) 'Turbulently flowing liquid – liquid dispersions . Part I : Drop breakage and coalescence', *Chemical Engineering Journal*. Elsevier B.V., 166(2), pp. 715–725. doi: 10.1016/j.cej.2010.11.050.

Azizi, F. and Al Taweel, A. M. M. (2011) 'Hydrodynamics of Liquid Flow Through Screens and Screen-Type Static Mixers', *Chemical Engineering Communications*, 198(5), pp. 726–742. doi: 10.1080/00986445.2011.532748.

Bansode, S. S., Banarjee, S. K., Gaikwad, D. D., Jadhav, S. L. and Thorat, R. M. (2012)

'Microencapsulation : A Review', *International Journal of Pharmaceutical Sciences Review and Research*, 1(2), pp. 509–531.

Das, M. D., Hrymak, A. N. and Baird, M. H. I. (2013) 'Laminar liquid – liquid dispersion in the SMX static mixer', *Chemical Engineering Science*. Elsevier, 101, pp. 329–344. doi: 10.1016/j.ces.2013.06.047.

Das, P. K., Legrand, J., Morançais, P. and Carnelle, G. (2005) 'Drop breakage model in static mixers at low and intermediate Reynolds number', 60, pp. 231–238. doi: 10.1016/j.ces.2004.08.003.

Dobetti, L. and Pantaleo, V. (2002) 'Application of a hydrodynamic model to microencapsulation by coacervation.', *Journal of microencapsulation*, 19(2), pp. 139–151. doi: 10.1080/02652040110055199.

Farzi, G. A., Rezazadeh, N. and Nejad, A. P. (2016) 'Droplet Formation Study in Emulsification Process by KSM using a Novel In Situ Visualization System', *Journal of Dispersion Science and Technology*, 37(4). doi: 10.1080/01932691.2015.1052144.

Farzi, G., Mortezaei, M. and Badiei, A. (2010) 'Relationship Between Droplet Size and Fluid Flow Characteristics in Miniemulsion Polymerization of Methyl Methacrylate'. doi: 10.1002/app.

Fradette, L., Tanguy, P., Li, H. and Choplin, L. (1996) 'LIQUID / LIQUID VISCOUS DISPERSIONS WITH A SMX STATIC MIXER', *Chemical Engineering Research and Design*, 85(2), pp. 395–405. doi: 10.1205/cherd06206.

Gupta, A. and Dey, B. (2013) 'Microencapsulation for controlled drug delivery: a comprehensive review', *Sunsari Technical College Journal*, 1(1), pp. 48–54. doi: 10.3126/stcj.v1i1.8660.

Hessel, V. (2009) 'Process windows - gate to maximizing process intensification via

flow chemistry', *Chemical Engineering and Technology*, pp. 1655–1681. doi: 10.1002/ceat.200900474.

Hobbs, D. M. and Muzzio, F. J. (1997) 'The Kenics static mixer: A three-dimensional chaotic flow', *Chemical Engineering Journal*, 67(3), pp. 153–166. doi: 10.1016/S1385-8947(97)00013-2.

Hobbs, D. M. and Muzzio, F. J. (1998) 'Reynolds number effects on laminar mixing in the Kenics static mixer', *Chemical Engineering Journal*, 70(2), pp. 93–104. doi: 10.1016/S1385-8947(98)00065-5.

Hweij, K. A. and Azizi, F. (2015) 'Hydrodynamics and residence time distribution of liquid flow in tubular reactors equipped with screen-type static mixers', *CHEMICAL ENGINEERING JOURNAL*. Elsevier B.V., 279, pp. 948–963. doi: 10.1016/j.cej.2015.05.100.

Jensen, K. (2001) 'Microreaction engineering—is small better?', *Chemical Engineering Science, 2001*, 56, pp. 293–303. doi: 10.1016/S0009-2509(00)00230-X.

Jeong, H. H., Issadore, D. and Lee, D. (2016) 'Recent developments in scale-up of microfluidic emulsion generation via parallelization', *Korean Journal of Chemical Engineering*, 33(6), pp. 1757–1766. doi: 10.1007/s11814-016-0041-6.

Jyothi, N. V. N., Prasanna, P. M., Sakarkar, S. N., Prabha, K. S., Ramaiah, P. S. and Srawan, G. Y. (2010) 'Microencapsulation techniques, factors influencing encapsulation efficiency.', *Journal of microencapsulation*, 27(3), pp. 187–197. doi: 10.3109/02652040903131301.

Kiss, N., Brenn, G., Pucher, H., Wieser, J., Scheler, S., Jennewein, H., Suzzi, D. and Khinast, J. (2011) 'Formation of O / W emulsions by static mixers for pharmaceutical applications', *Chemical Engineering Science*. Elsevier, 66(21), pp. 5084–5094. doi:

10.1016/j.ces.2011.06.065.

Klutz, S., Kurt, S. K., Lobedann, M. and Kockmann, N. (2015) 'Narrow residence time distribution in tubular reactor concept for Reynolds number range of 10–100', *Chemical Engineering Research and Design*. Institution of Chemical Engineers, 95, pp. 22–33. doi: 10.1016/j.cherd.2015.01.003.

Kondo, A. and van Valkenburg, W. (1979) *Microcapsule Processing and Technology*. New York: Dekker.

Leal-Calderon, F., Schmitt, V. and Bibette, J. (2007) *Emulsion science, basic principles*. New York: Springer Science+Business Media. doi: 10.1007/978-0-387-39683-5.

Legrand, J. and Moranc, P. (2001) 'LIQUID – LIQUID DISPERSION IN AN', 79(November).

Levenspiel, O. (1999) *Chemical reaction engineering*. 3rd edn, *Chemical Engineering Science*. 3rd edn. New York. doi: 10.1016/0009-2509(64)85017-X.

Martin-Banderas, L., Ganan-Calvo, a. M. and Fernandez-Arevalo, M. (2010) 'Making Drops in Microencapsulation Processes', *Letters in Drug Design & Discovery*, 7(4), pp. 300–309. doi: 10.2174/157018010790945760.

Martín, M. J., Lara-Villoslada, F., Ruiz, M. A. and Morales, M. E. (2015) 'Microencapsulation of bacteria: A review of different technologies and their impact on the probiotic effects', *Innovative Food Science and Emerging Technologies*, 27, pp. 15–25. doi: 10.1016/j.ifset.2014.09.010.

Meijer, H. E. H., Singh, M. K. and Anderson, P. D. (2012) 'Progress in Polymer Science On the performance of static mixers : A quantitative comparison', *Progress in Polymer Science*. Elsevier Ltd, 37(10), pp. 1333–1349. doi: 10.1016/j.progpolymsci.2011.12.004.

Merline, D. J., Vukusic, S. and Abdala, A. A. (2013) 'Melamine formaldehyde: curing studies and reaction mechanism', *Polymer Journal*. Nature Publishing Group, 45(4), pp. 413–419. doi: 10.1038/pj.2012.162.

Nesterova, T., Dam-johansen, K. and Kiil, S. (2011) 'Progress in Organic Coatings Synthesis of durable microcapsules for self-healing anticorrosive coatings : A comparison of selected methods', *Progress in Organic Coatings*. Elsevier B.V., 70(4), pp. 342–352. doi: 10.1016/j.porgcoat.2010.09.032.

Nesterova, T., Dam-johansen, K., Thorslund, L. and Kiil, S. (2012) 'Progress in Organic Coatings Microcapsule-based self-healing anticorrosive coatings : Capsule size , coating formulation , and exposure testing', *Progress in Organic Coatings*. Elsevier B.V., 75(4), pp. 309–318. doi: 10.1016/j.porgcoat.2012.08.002.

Neves, M. A., Ribeiro, H. S., Fujiu, K. B., Kobayashi, I. and Nakajima, M. (2008) 'Formulation of Controlled Size PUFA-Loaded Oil-in-Water Emulsions by Microchannel Emulsification Using -Carotene-Rich Palm Oil', pp. 6405–6411.

Nguyen, L. T., Hillewaere, X. K. D., Teixeira, R. F. A., van den Berg, O. and Du Prez, F. E. (2015) 'Efficient microencapsulation of a liquid isocyanate with in situ shell functionalization', *Polym. Chem.* Royal Society of Chemistry, 6(7), pp. 1159–1170. doi: 10.1039/C4PY01448K.

Nisisako, T. and Torii, T. (2008) 'Microfluidic large-scale integration on a chip for mass production of monodisperse droplets and particles {', pp. 287–293. doi: 10.1039/b713141k.

Nisisako, T., Torii, T. and Higuchi, T. (2002) 'Droplet formation in a microchannel network †', pp. 24–26. doi: 10.1039/b108740c.

Paul, E. L., Atiemo-obeng, V. a and Kresta, S. M. (2004) *HANDBOOK OF*

INDUSTRIAL MIXING Edited by. doi: 10.1002/0471451452.

Rodrigues, S. N., Martins, I. M., Fernandes, I. P., Gomes, P. B., Mata, V. G., Barreiro, M. F. and Rodrigues, A. E. (2009) 'Scentfashion(R): Microencapsulated perfumes for textile application', *Chemical Engineering Journal*, 149(1–3), pp. 463–472. doi: 10.1016/j.cej.2009.02.021.

Schrooyen, P. M., van der Meer, R. and De Kruif, C. G. (2001) 'Microencapsulation: its application in nutrition.', *The Proceedings of the Nutrition Society*, 60(4), pp. 475–479. doi: 10.1079/PNS2001112.

Al Shannaq, R. and Farid, M. M. (2015) *Microencapsulation of phase change materials (PCMs) for thermal energy storage systems*, *Advances in Thermal Energy Storage Systems*. Woodhead Publishing Limited. doi: 10.1533/9781782420965.2.247.

Singh, M. N., Hemant, K. S. Y., Ram, M. and Shivakumar, H. G. (2010) 'Microencapsulation: A promising technique for controlled drug delivery', *Research in Pharmaceutical Sciences*, 5(2), pp. 65–77.

Sugiura, S., Nakajima, M. and Seki, M. (2002) 'Effect of channel structure on microchannel emulsification', *Langmuir*, 18(15), pp. 5708–5712. doi: 10.1021/la025813a.

Thakur, R., Vial, C. and Nigam, K. (2003) 'Static mixers in the process industries—a review', *Research and Design*, 81(7), pp. 787–826. doi: 10.1205/026387603322302968.

Then, S., Seng Neon, G. and Abu Kasim, N. H. (2011) 'Optimization of Microencapsulation Process for Self-Healing Polymeric Material', 40(7), pp. 795–802.

Theron, F., Anxionnaz-Minvielle, Z., Le Sauze, N. and Cabassud, M. (2012) 'Transposition from a batch to a continuous process for microencapsulation by interfacial polycondensation', *Chemical Engineering and Processing: Process*

Intensification. Elsevier B.V., 54, pp. 42–54. doi: 10.1016/j.cep.2012.01.001.

Theron, F. and Sauze, N. Le (2011) 'Comparison between three static mixers for emulsification in turbulent flow', *International Journal of Multiphase Flow*. Elsevier Ltd, 37(5), pp. 488–500. doi: 10.1016/j.ijmultiphaseflow.2011.01.004.

Theron, F., Le Sauze, N. and Ricard, A. (2010) 'Turbulent liquid-liquid dispersion in sulzer SMX mixer', *Industrial and Engineering Chemistry Research*. doi: 10.1021/ie900090d.

Tucker III, C. L. and Moldenaers, P. (2002) 'M ICROSTRUCTURAL E VOLUTION IN P OLYMER B LENDS', pp. 177–210.

Vladisavljević, G. T., Kobayashi, I. and Nakajima, M. (2012) 'Production of uniform droplets using membrane, microchannel and microfluidic emulsification devices', *Microfluidics and Nanofluidics*, 13(1), pp. 151–178. doi: 10.1007/s10404-012-0948-0.

Wagdare, N. A., Marcelis, A. T. M., Ho, O. B., Boom, R. M. and van Rijn, C. J. M. (2010) 'High throughput vegetable oil-in-water emulsification with a high porosity micro-engineered membrane', *Journal of Membrane Science*, 347(1–2), pp. 1–7. doi: 10.1016/j.memsci.2009.09.057.

Wiles, C. and Watts, P. (2008) 'Continuous flow reactors, a tool for the modern synthetic chemist', *European Journal of Organic Chemistry*, (10), pp. 1655–1671. doi: 10.1002/ejoc.200701041.

Wischke, C., Lorenzen, D., Zimmermann, J. and Borchert, H. (2006) 'Preparation of protein loaded poly (D , L -lactide-co-glycolide) microparticles for the antigen delivery to dendritic cells using a static micromixer', 62, pp. 247–253. doi: 10.1016/j.ejpb.2005.08.015.

Wu, D. Y., Meure, S. and Solomon, D. (2008) 'Self-healing polymeric materials: A

review of recent developments', *Progress in Polymer Science*, 33(5), pp. 479–522. doi: 10.1016/j.progpolymsci.2008.02.001.

Yamazaki, N., Yuyama, H., Nagai, M., Ma, G.-H. and Omi, S. (2002) 'A Comparison of Membrane Emulsification Obtained Using SPG (Shirasu Porous Glass) and PTFE [Poly(Tetrafluoroethylene)] Membranes', *Journal of Dispersion Science and Technology*, 23(January 2014), pp. 279–292. doi: 10.1080/01932690208984204.

Yuyama, H., Watanabe, T., Ma, G. H., Nagai, M. and Omi, S. (2000) 'Preparation and analysis of uniform emulsion droplets using SPG membrane emulsification technique', *Colloids and Surfaces A: Physicochemical and Engineering Aspects*, 168(2), pp. 159–174. doi: 10.1016/S0927-7757(00)00452-0.

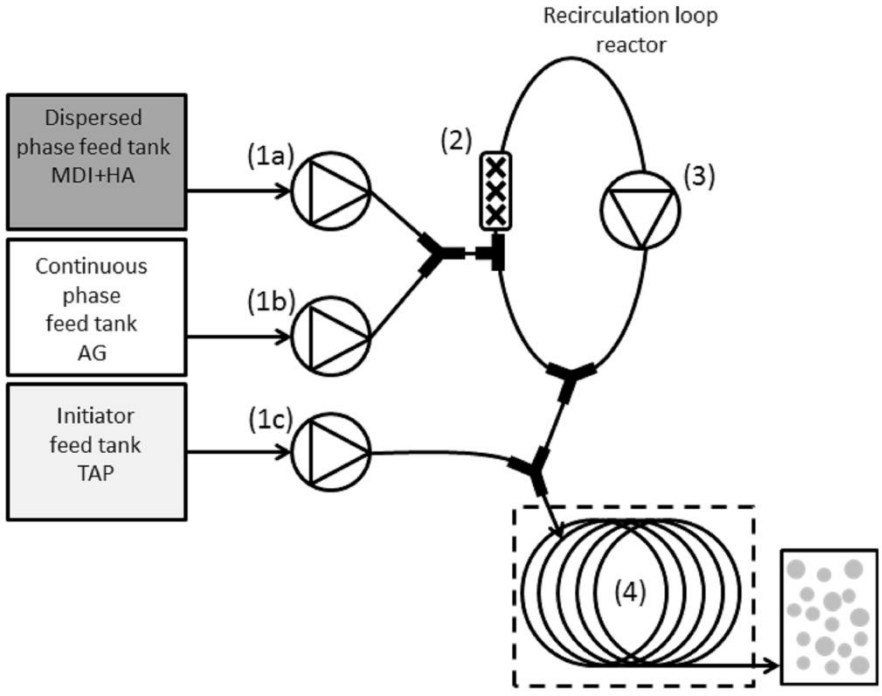

Figure 1: Schematic representation of flow setup with post emulsification addition of TAP.

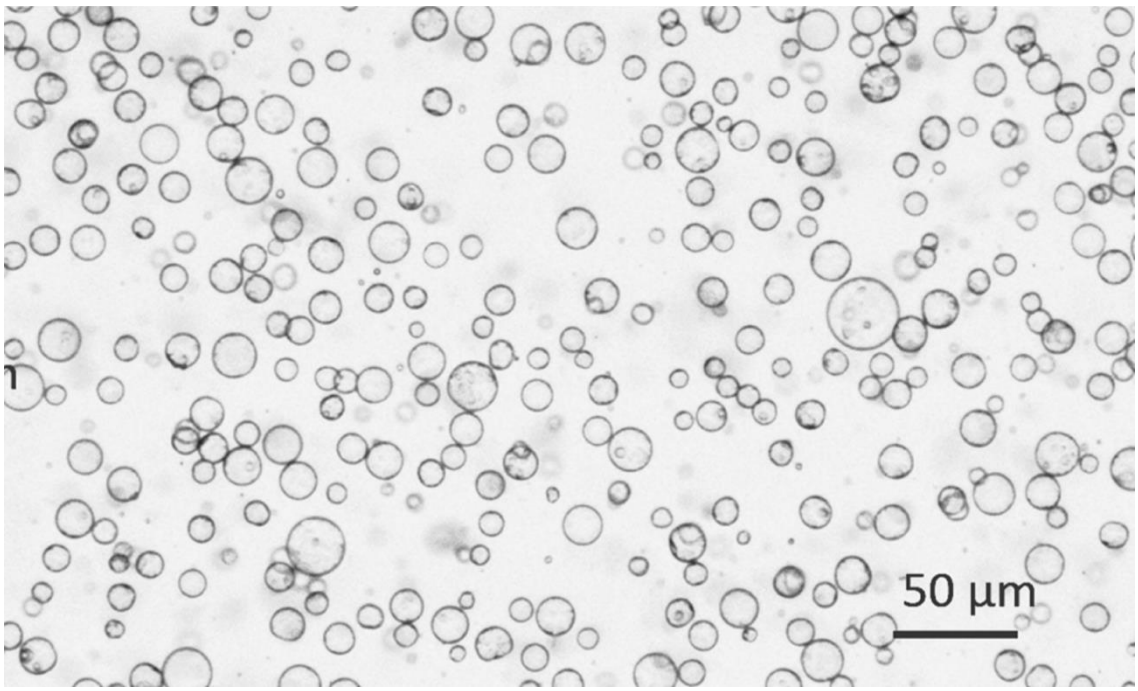

Figure 2: Microcapsules generated at 0.31 m/s and 13 Kenics® static mixer in a recirculation loop driven by a peristaltic pump.

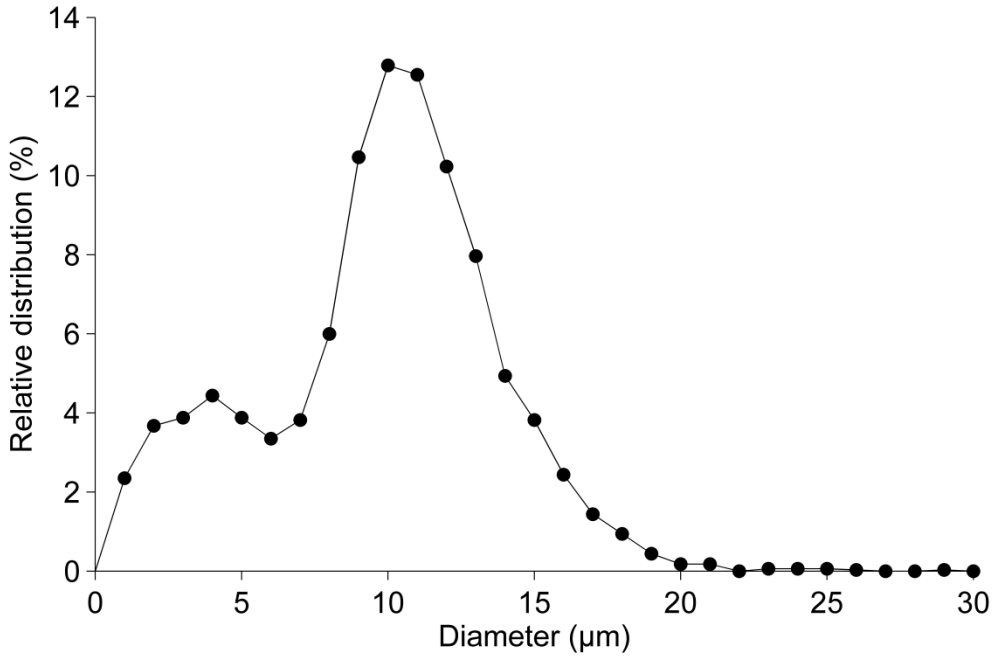

Figure 3: Number based CSD of batch produced microcapsules with a high shear mixer at 7600 rpm.

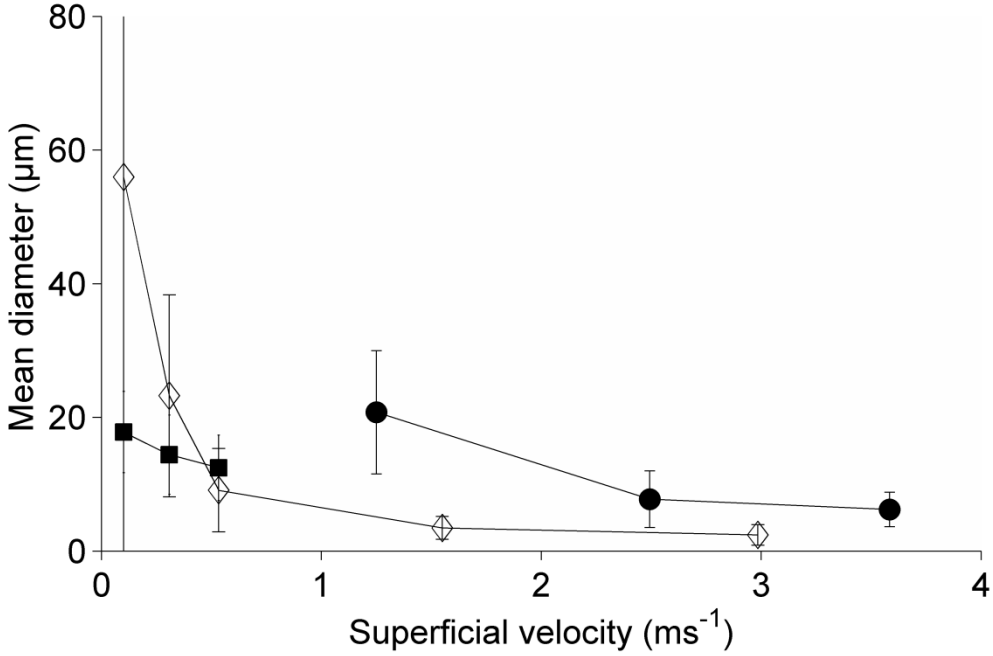

Figure 4: Mean diameter and covariance of CSD obtained in a recirculation loop operated with a peristaltic (■), centrifugal (●) or gear pump (◊).The error bars indicate the spread of the capsule size distribution curves.

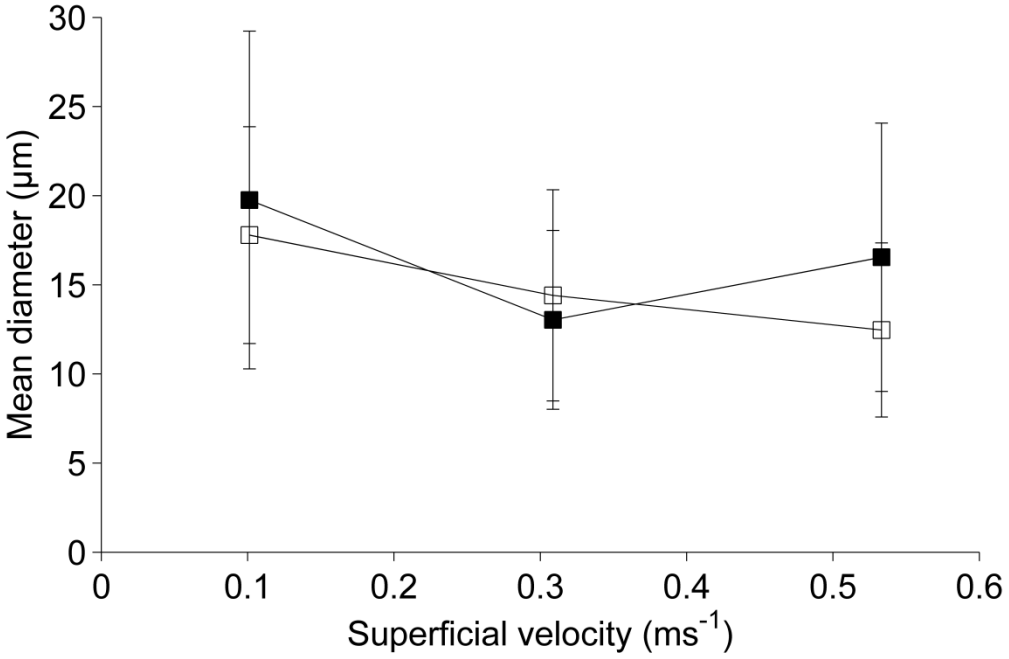

Figure 5: Mean diameter and covariance of microcapsules produced in a recirculation loop with peristaltic pump at v = 0.1, 0.31, 0.53m/s, with pre-emulsification (□), or post-emulsification (■) addition of TAP. The error bars indicate the spread of the capsule size distribution curves.

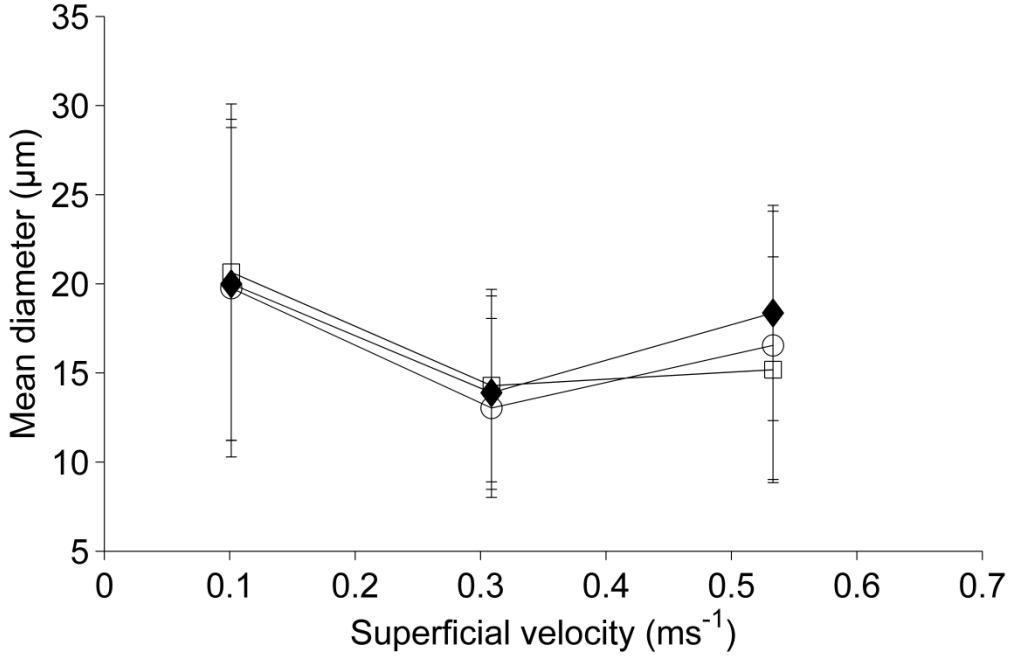

Figure 6: Mean diameter and covariance of capsule size distributions obtained in a recirculation loop fitted with 13 Kenics® static mixer's (□), or 9 screen type mixers, (♦), operated with a peristaltic pump and post emulsification addition of TAP. The results of capsules generated without static mixers are indicated by (○).

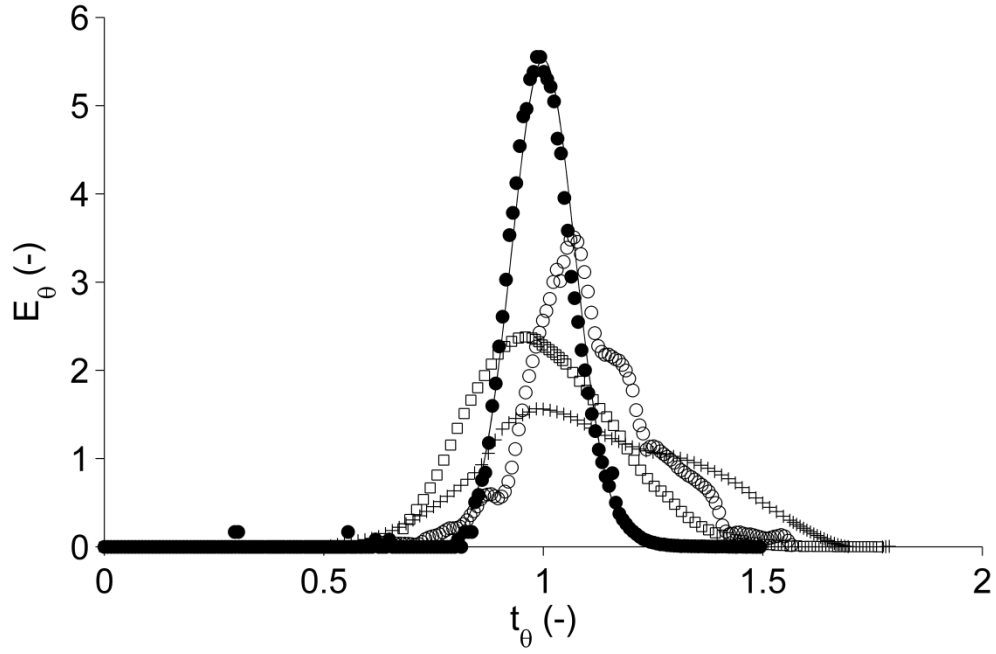

Figure 7: Normalized residence time distribution curves obtained with RTD measurements of a single coiled tubular reactor with water (□) and emulsion (+) as the matrix, and an 8-shaped coil with water (●) and emulsion (○) as the matrix. The dispersion model (─) is based on the results of the 8-shaped coil with a water matrix.

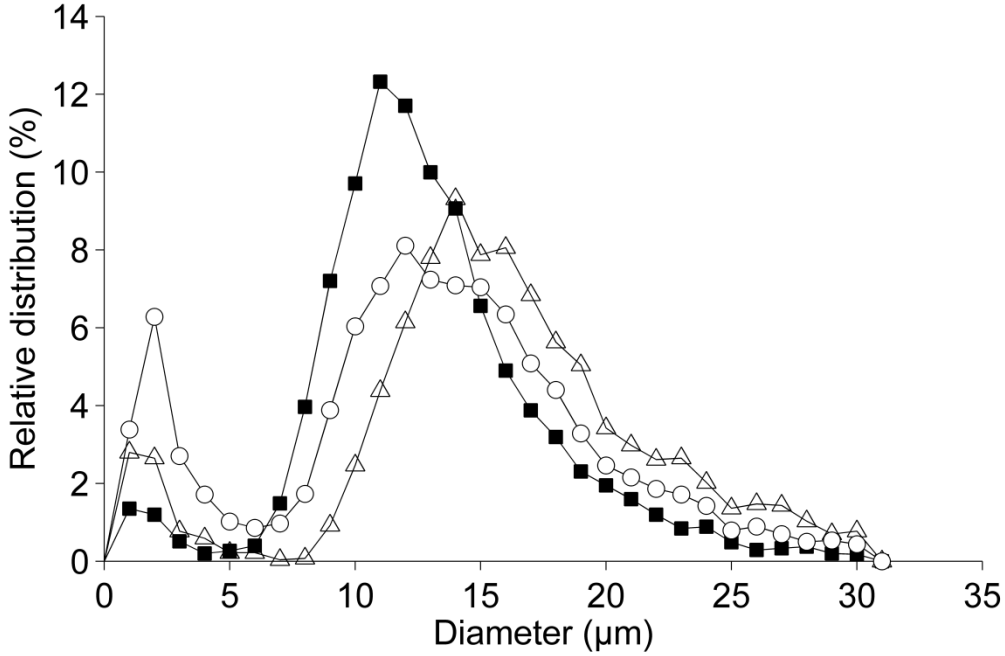

Figure 8: Capsules size distributions of capsules generated at 0.31 m/s with 13 Kenics® static mixer and cured in a single coiled tube (Δ), an 8-shaped coiled tube (○) and in batch (■).

Table 1: Overview of process parameters of continuous emulsification devices.

Reference	Mixing	Flow rate of encapsulated phase (L/h)	$\phi_{emulsion}$ (%)	Mean diameter (µm)	CoV (%)
Current work	Recirculation loop reactor	0.04	28.8	14.3	37.8
(Fradette *et al.*, 1996)	SMX	11.94	5.7	194	21.13
(Wischke *et al.*, 2006)	Micromixer	0.06	3.8	3.06	>20

(Neves *et al.*, 2008)	Micro channel emulsification	0.004	11.9	28.5	3.3
(Yuyama *et al.*, 2000)	Membrane emulsification (SPG)	0.9	4.7	<17	11-22
(Nisisako, Torii and Higuchi, 2002)	Micro fluidics	0.0015	5.2	100	1.3%